Available online at www.sciencedirect.com
SCIENCE DIRECT®
C. R. Chimie 8 (2005) 985–992
COMPTES RENDUS CHIMIE
http://france.elsevier.com/direct/CRAS2C/

Synthesis and electrochemistry of adducts of acetylene and acetylenedicarboxylic acid at sulfurs in sulfur-bridged nitrilotriacetato molybdenum clusters

Hideaki Takagi [a,*], Yasuhiro Ide [b], Takashi Shibahara [b,*]

[a] *Department of International Conservation Studies for Cultural Properties, Kibi International University, Igamachi 8, Takahashi-shi, Okayama 716-8508, Japan*
[b] *Department of Chemistry, Okayama University of Science, Ridai-cho, Okayama 700-0005, Japan*

Received 16 July 2004; accepted after revision 4 October 2004

Available online 17 February 2005

Abstract

Acetylene- and acetylenedicarboxylic acid (ADA) adducts were synthesized and characterized of sulfur-bridged trinuclear molybdenum clusters, $[Mo_3(\mu_3\text{-}S)(\mu\text{-}S)(\mu_3\text{-}SCH{=}CHS)(Hnta)_3]^{2-}$ (**2**) and $[Mo_3(\mu_3\text{-}S)(\mu\text{-}SC(COOH){=}CH(COOH))(\mu_3\text{-}SC(COOH){=}C(COOH)S)(Hnta)_3]^{-}$ (**3**) obtained through the reaction of $[Mo_3(\mu_3\text{-}S)(\mu\text{-}S)_3(Hnta)_3]^{2-}$ (**1**) with the above reagents, respectively. X-ray crystallography of K_2[**2**]·KCl·8 H_2O (**2′**) revealed the existence of two C–S bonds and indicated that the distance of the C–C moiety derived from acetylene is close to that of ethylene (1.33(2) Å). A cyclic voltammogram of **2** showed a one-electron oxidation process, which was not observed in **1**. In the reduction side, no appreciable change of the reduction potential was observed in the adduct formation. The clusters **2** and **3** were characterized by ^{1}H NMR and electronic spectroscopy, and the formation mechanism of **3** is discussed, where two kinds of intermediates are proposed: one has two C–S bonds, and the other, one C–S bond, which is caused by the scission with H^+. ***To cite this article: H. Takagi et al., C. R. Chimie 8 (2005).***
© 2005 Académie des sciences. Published by Elsevier SAS. All rights reserved.

Keywords: Acetylene adduct; Acetylenedicarboxylic acid; C–S bond formation; Sulfur-bridge; Molybdenum cluster; Electrochemistry

1. Introduction

Research on the formation and scission of carbon–sulfur bonds is important for the petrochemical industry in the field of vulcanization and for the elucidation of materials that play indispensable roles in the origin of life and living organisms. Dinuclear molybdenum complexes have been reported to catalyze the formation and scission of carbon–sulfur bonds [1].

Incomplete cubane-type molybdenum and tungsten clusters are also targets of research relative to the formation and scission of carbon–sulfur bonds. The sulfur-bridged aqua cluster $[Mo_3(\mu_3\text{-}S)(\mu\text{-}S)_3(H_2O)_9]^{4+}$ reacts with acetylene to give the adduct $[Mo_3(\mu_3\text{-}S)(\mu\text{-}S)(\mu_3\text{-}SCH{=}CHS)(H_2O)_9]^{4+}$. In addition, the reaction of tungsten clusters having $W_3(\mu_3\text{-}S)(\mu\text{-}X)(\mu\text{-}S)_2$ cores (X = O, S) with acetylene and its derivatives has also been reported (Scheme 1) [2–4]. Every adduct formation resulted in a large electronic spectral transformation, which indicates a large change in the electronic state of the $M_3(\mu_3\text{-}S)(\mu\text{-}X)(\mu\text{-}S)_2$ (M = Mo, W; X = O, S) core.

* Corresponding authors.
E-mail addresses: takagi@kiui.ac.jp (H. Takagi), shiba@chem.ous.ac.jp (T. Shibahara).

1631-0748/$ - see front matter © 2005 Académie des sciences. Published by Elsevier SAS. All rights reserved.
doi:10.1016/j.crci.2004.10.031

These results indicate that the reactivity of the clusters towards acetylene or its derivatives varies considerably with changes in metals, bridging atoms, and/or ligands.

The nitrilotriacetato molybdenum cluster, $[Mo_3(\mu_3\text{-}S)(\mu\text{-}S)_3(Hnta)_3]^{2-}$ (**1**), is stable in the pH 2–11 region, and three consecutive one-electron reduction processes of **1** have been reported together with a one-electron reduced mixed-valence cluster [5]. As for the aqua cluster $[Mo_3(\mu_3\text{-}S)(\mu\text{-}S)_3(H_2O)_9]^{4+}$, the hydrogen evolution prevented the measurement of the reduction potentials. We report here on the synthesis and characterization of adducts of acetylene and acetylenedicarboxylic acid (ADA) at sulfurs in the sulfur-bridged incomplete cubane-type molybdenum **1** in water. This

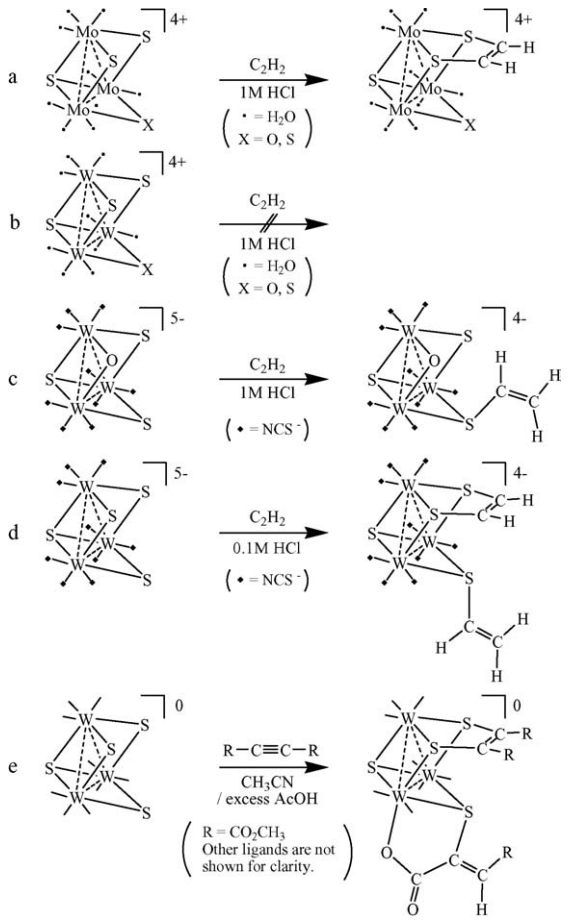

Scheme 1. Reaction of sulfur-bridged clusters with acetylene. (a) $[Mo_3(\mu_3\text{-}S)(\mu\text{-}X)(\mu\text{-}S)_2(H_2O)_9]^{4+}$ (X = O, S) (b) $[W_3(\mu_3\text{-}S)(\mu\text{-}X)(\mu\text{-}S)_2(H_2O)_9]^{4+}$ (X = O, S) (c) $[W_3(\mu_3\text{-}S)(\mu\text{-}O)(\mu\text{-}S)_2(NCS)_9]^{5-}$, (d) $[W_3(\mu_3\text{-}S)(\mu\text{-}S)_3(NCS)_9]^{5-}$, and (e) $W_3(\mu_3\text{-}S)(\mu\text{-}S)_3(dtp)_3(\mu\text{-}OAc)(CH_3CN)$].

is, to our knowledge, the first report on the electrochemistry of acetylene (or its derivatives) adducts of trinuclear clusters.

2. Experimental

2.1. Materials and reagents

All the chemicals were obtained from commercial sources and used as received. Cluster **1** was prepared according to the literature [6].

2.2. Synthesis

2.2.1. Synthesis of $K_2[Mo_3(\mu_3\text{-}S)(\mu\text{-}S)(\mu_3\text{-}SCH{=}CHS)(Hnta)_3]\cdot KCl\cdot 8\ H_2O$ (**2′**)

Raising the pH of a slurry of $K_2[Mo_3(\mu_3\text{-}S)(\mu\text{-}S)_3(Hnta)_3]\cdot 9\ H_2O$ (**1′**) (199.6 mg, 0.163 mmol) in water (5 ml) to ca. 7 by the addition of 4 M KOH turned the slurry into a solution. Acetylene was passed through the resultant solution for 10 min, which caused the solution to change from green to deep green. The pH of the solution was adjusted to 1.2 by the addition of 2 M HCl. The addition of KCl (74.6 mg, 1.0 mmol) and the filtration of the solution were followed by passing acetylene for another 10 min, and the solution was sealed. Storage of the solution in a refrigerator at 2 °C overnight resulted in green needle-like crystals of **2′** with a yield of 85.8 mg (40.3%). Anal. Found (Calc. for $Mo_3S_4K_3ClO_{26}N_3C_{20}H_{39}$)%: C, 18.43 (18.39); H, 2.89 (3.01); N, 3.18 (3.22).

2.2.2. Synthesis of $K[Mo_3(\mu_3\text{-}S)(\mu\text{-}SC(COOH){=}CH(COOH))(\mu_3\text{-}SC(COOH){=}C(COOH)S)(Hnta)_3]\cdot 8\ H_2O$ (**3′**)

The same procedures that were used in the synthesis of **2′** were followed up to the addition of a small amount of 4 M KOH to the slurry of **1′** (50 mg, 40 μmol) in water (5 ml) to give a pH 7 solution. The addition of ADA (5.56 mg, 49 μmol) with stirring caused the solution to change from deep green to greenish brown. The pH of the solution was adjusted to 1.2 by the addition of 2 M HCl. Storage of the solution in a refrigerator at 2 °C overnight resulted in brown needle-like crystals of **3′** with a yield of 76.26 mg (46.38%). Anal. Found (Calc. for $Mo_3S_4KO_{32}N_3C_{26}H_{45}$)%: C, 22.30 (22.37); H, 3.28 (3.03); N, 3.20 (3.01).

2.3. Measurements of electronic spectra

Electronic spectra were measured using a Hitachi U-2000 double-beam spectrometer in a 10-mm quart

cell sealed with Septa® rubber at room temperature in the 340–1100-nm region.

*2.3.1. Reaction of **1′** with acetylene*

The electronic spectrum of **1′** (5.0 mg, 4.0 μmol) in water (5 ml) was measured, and acetylene gas was passed through the solution for 5 min. The color of the solution changed from green to deep green. The electronic spectrum of the resultant solution was measured immediately.

*2.3.2. Reaction of **1′** with ADA at pH 1.2*

The electronic spectrum of **1′** (5.4 mg, 4.1 μmol) in water (5 ml) was measured, and ADA (1.20 mg, 10.5 μmol) was added to the solution. An immediate color change of the solution was observed from green to deep green. Two- and one-half hours after the addition of ADA, the absorption at 853 nm reached its maximum, and the pH was measured (pH 2.6). The pH of the solution was then adjusted to 1.2, and the electronic spectrum of the resultant solution was measured immediately and 6, 12, 18.5, 24.5, 30.5, 36.5, 42.4 and 65.5 h after pH adjustment to 1.2. The color of the resultant solution turned gradually from deep green to greenish brown.

*2.3.3. Reaction of **1′** with ADA at pH 9*

The reaction of **1′** with ADA was followed as described in Section 2.2.2, except that the pH of the reaction mixture was adjusted to nine just after the addition of ADA to the solution of **1′**. The spectra of the solution were measured intermittently.

2.4. Measurements of ^{1}H NMR spectra and electrochemistry

^{1}H NMR spectra of samples in D_2O were obtained at 20 °C with a Bruker ARX-400R spectrometer. 3-(Trimethylsilyl)-1-propanesulfonic acid, sodium salt (DSS) = 0.0 ppm. Cyclic voltammetry of the molybdenum clusters was performed either in a phthalic solution (0.5 mM, pH 4.1) or in a phosphate solution (0.5 mM, pH 7.0) with a BAS 100W electrochemical analyzer. The working electrode was a glassy carbon disc (φ = 3.0 mm). The reference and counter electrodes were Ag/AgCl (3 M NaCl) and a platinum wire, respectively. Supporting electrolyte was Na_2SO_4 (0.1 M). All the solutions were deoxygenated with a stream of argon prior to each run.

*2.5. Structural determination of $K_2[Mo_3(\mu_3\text{-}S)(\mu\text{-}S)(\mu_3\text{-}SCH{=}CHS)(Hnta)_3]\cdot KCl\cdot 8\ H_2O$ (**2′**)*

X-ray diffraction data were collected with a Rigaku CCD diffractometer and analyzed using the teXsan system. A single crystal of **2′** was mounted on the tip of a glass fiber and cooled to –160 °C. The dimensions were 0.20 × 0.10 × 0.01 mm. The structure was solved by the direct (SIR92) [7] and Patterson methods (DIRDIF94) [8], and all the remaining non-hydrogen atoms were located from difference maps. All hydrogen atoms were assigned to idealized positions (C–H 1.09 Å, HC=CH 1.08 Å) with thermal parameters that were 1.2 times the thermal parameters of the carbon atoms to which each was attached. All the calculations were performed using the teXsan crystallographic software package [9].

The crystal data and structure refinement parameters are listed in Table 1. All pertinent crystallographic information for the cluster, including bond distances and angles, atomic coordinates, and equivalent isotropic displacement parameters, is provided in the Supporting Information.

3. Results and discussion

*3.1. Synthesis of clusters **2′** and **3′***

Hnta clusters **1′**, **2′**, and **3′** are difficult to dissolve in acidic water but not in neutral water because of the dissociation of some of the three –COOH groups in each cluster. At strong acidity, e.g. 1 M HCl, a dissociation of Hnta ligands occurs. Accordingly, for the synthesis of **2′** and **3′**, we first raised the pH to ca. 7 with KOH to dissolve **1′**, adjusted the pH to 1.2 with HCl after the adduct formation, and attained moderate yields for both clusters. Without the addition of KCl, the yield of **2′** was lower (ca. 14%). The formation of the double salt, **2′**, from $K_2[Mo_3(\mu_3\text{-}S)(\mu\text{-}S)(\mu_3\text{-}SCH{=}CHS)(Hnta)_3]$ (K_2**2**) and KCl probably reduced the solubility of K_2**2**.

*3.2. Electronic spectral change on the formation of clusters **2** and **3***

The spectral change on passing acetylene through the solution of **1** indicated the formation of **2**, which had a large peak in the near infrared region, as shown

Table 1
Crystallographic data for $K_2[Mo_3(\mu\text{-}S)(\mu_3\text{-}S)(\mu_3\text{-}SCH{=}CHS)(Hnta)_3]\cdot KCl\cdot 8\,H_2O$ (**2′**)

Compound	**2′**
Formula	$Mo_3K_3ClS_4O_{26}N_3C_{20}H_{39}$
Formula weight	1306.34
Crystal color, habit	Green, plate
Crystal dimensions (mm)	0.20 × 0.10 × 0.01
Crystal system	Monoclinic
Space group	*C*2/*c* (No.15)
a (Å)	22.953(3)
b (Å)	21.044(2)
c (Å)	18.542(2)
β (°)	114.962(3)
V (Å^3)	8119(1)
Z	8
Diffractometer	Rigaku/MSC mercury CCD
R_1[a]	0.089
R, R_w[b]	0.156 (0.254)
Goodness of fit indicator[c]	1.03
D_{calc} (g/cm^3)	2.137
μ (cm^{-1})	15.86
No. of measured reflections	42858
No. of unique reflections (R_{int} = 0.087)	9102
No. of observed reflections	9102 (all data)
No. of variables	541
Data: parameter ratio	16.82
Temperature (°C)	–180.0

[a] $R_1 = \Sigma||F_o| - |F_c||/\Sigma|F_o|$ for $I > 2\sigma(I)$.
[b] $R = \Sigma(F_o^2 - F_c^2)/\Sigma F_o^2$, $R_w(F_o^2) = [\Sigma w(F_o^2 - F_c^2)^2/\Sigma w(F_o^2)^2]^{1/2}$ where $w = \sigma_c^2(F_o^2)^{-1} = [\sigma_c^2(F_o^2) + (p(\mathrm{Max}(F_o^2, 0) + 2F_c^2)/3)^2]^{-1}$, $P = 0.090$.
[c] Goodness of fit indicator = $[\Sigma w(F_o^2 - F_c^2)^2/(N_{observations} - N_{variables})]^{1/2}$.

in Fig. 1 (λ_{max}/nm, ϵ/M^{-1}cm^{-1}), 458sh (974), 654 (764), 890 (1889)). The resultant spectrum changed very slightly in the air. The spectral change was more complicated when the reaction of **1** with ADA proceeded to give **3**. The absorption peak at 853 nm of the reaction mixture (pH 2.6) increased gradually for two- and one-half hours, and then the spectral change became small. Addition of hydrochloric acid, however, to adjust pH to 1.2 resulted in a large spectral change, and, finally, the spectrum approached that of **3**, with the peak at 853 nm gradually disappearing. The spectral change is shown in Fig. 2. The reaction of **1** with ADA at pH 9 was much slower. The absorption peak at 853 nm reached its maximum 11 h after the mixing, and the peak height remained unchanged. If acid is added at this point, the peak height starts to decrease, indicating

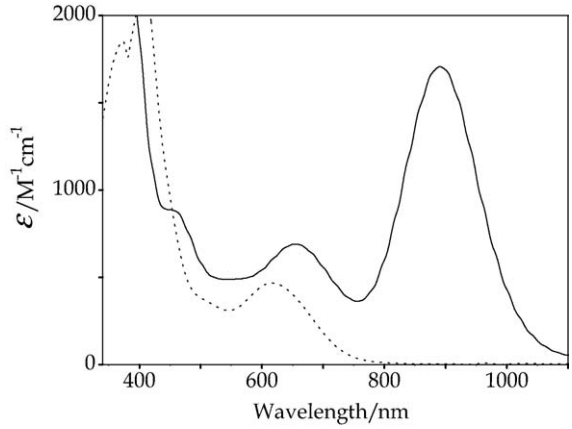

Fig. 1. Electronic spectra of **1′** (---) and **2′** (——).

the formation of **3**. When dissociation constants of ADA (pK_{a1} = 1.74, pK_{a2} = 4.38) are taken into consideration, the reactivity of dissociated ADA toward the μ-S of **1** is lower than that of the undissociated species.

3.3. X-ray structure of 2′

The X-ray structural analysis of **2′** clearly revealed the formation of the two carbon–sulfur bonds, as shown in Fig. 3. The interatomic distances and angles are listed in Tables 2 and 3, respectively. Some of the dimensions of the cluster anion are clearly different from those of **1** in $Na_2[Mo_3S_4(Hnta)_3]\cdot 5H_2O$ (**1″**) [10].

Elongation of all six Mo-μ-S distances was observed on the adduct formation. The four Mo-μ-S′ distances

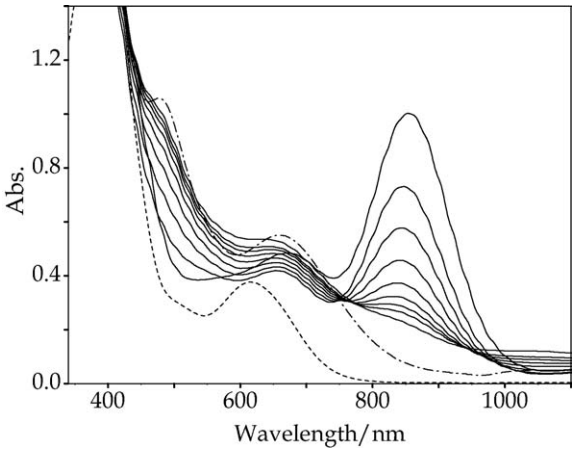

Fig. 2. Electronic spectral changes in reaction of **1** with ADA immediately and 6, 12, 18.5, 24.5, 30.5, 36.5, 42.4 and 65.5 h after pH adjustment to 1.2. **1′** (---), **3′** (–·–).

(S′: at the bridging sulfur atoms the adduct formation occurred) are in the range of 2.359(3)–2.444(3) Å, and the two Mo-μ-S distances are in the range of 2.317(3)–2.319(3) Å, while the six Mo-μ-S distances of **1″** are in the range of 2.272(2)–2.309(2) Å. On the other hand, little change was observed in three Mo-μ_3-S distances on the adduct formation: 2.317(3)–2.347(3) Å in **2′** and 2.330(2)–2.338(2) Å in **1″**. The carbon–carbon distance (C1–C2, 1.33(2) Å) was closer to that of ethylene (1.339 Å) than to that of acetylene (1.203 Å), and the bond angles at about C1 and C2 are close to 120° (S2–C1–C2, 121.4(9)°; S2–C2–C1, 122.1(9)°). The C–S bonds (C1–S2, 1.80(1) Å; C2–S4, 1.81(1) Å) are close to those in the aqua cluster $[Mo_3(\mu_3\text{-}S)(\mu\text{-}O)(\mu_3\text{-}SCH{=}CHS)(H_2O)_9]^{4+}$ [2].

3.4. ^{1}H NMR spectra of clusters 2′ and 3′

^{1}H NMR spectra of **2′** and **3′** in D_2O are shown in Fig. 4. The signal of **2′** at 6.28 (2H, s) ppm is assignable to the μ_3-SCH=CHS moiety. The very weak signal of **2′** at 2.30 (s) ppm is assignable to free acetylene. The dissociation of acetylene is also perceived through the slow decrease of the peak at 890 nm in the electronic spectrum of **2′**.

The signal of **3′** at 7.37 (1H, s) ppm is assignable to the μ-SCR=CRH moiety, which confirms the proton addition (see formation mechanism). The conformation of the moiety in **3′**, which is depicted in the inserted structure, was suggested by that of $[W_3(\mu_3\text{-}S)(\mu_3\text{-}SCR{=}CRS)(\mu\text{-}SCR{=}CRH)(NCS)_9]^{4-}$ [4]. The signals in the 3.0–6.0 region are due to methylenic protons of Hnta's of **2′** and **3′**.

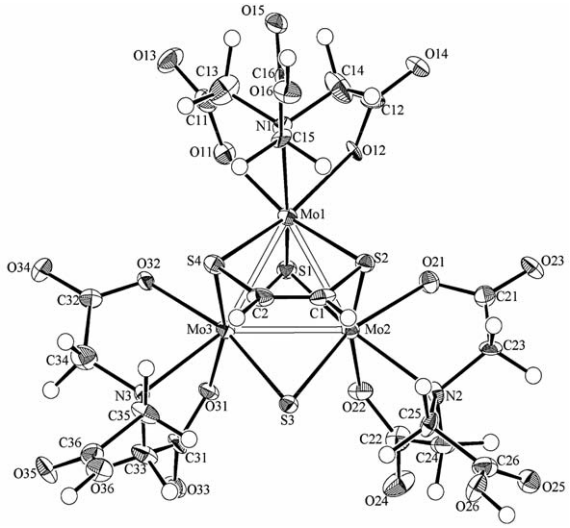

Fig. 3. ORTEP drawing of the anion of **2′**.

Table 2
Bond lengths in $K_2[Mo_3(\mu\text{-}S)(\mu_3\text{-}S)(\mu_3\text{-}SCH{=}CHS)(Hnta)_3]\cdot KCl\cdot 8H_2O$ (**2′**)

Atom	Atom	Length (Å)	Atom	Atom	Length (Å)
Mo1	Mo2	2.763(1)	Mo1	Mo3	2.749(1)
Mo2	Mo3	2.667(1)	Mo1	S1	2.317(3)
Mo1	S2	2.376(3)	Mo1	S4	2.359(3)
Mo2	S1	2.341(3)	Mo2	S2	2.444(3)
Mo2	S3	2.319(3)	Mo3	S1	2.347(3)
Mo3	S3	2.317(3)	Mo3	S4	2.424(3)
Mo1	O11	2.124(7)	Mo1	O12	2.133(7)
Mo2	O21	2.118(7)	Mo2	O22	2.092(8)
Mo3	O31	2.111(7)	Mo3	O32	2.120(7)
Mo1	N1	2.344(9)	Mo2	N2	2.333(8)
Mo3	N3	2.327(8)	S2	C1	1.80(1)
S4	C2	1.81(1)	O11	C11	1.28(1)
O13	C11	1.25(1)	O12	C12	1.29(1)
O14	C12	1.23(1)	O15	C16	1.22(1)
O16	C16	1.33(1)	O21	C21	1.30(1)
O23	C21	1.23(1)	O22	C22	1.28(1)
O24	C22	1.25(1)	O25	C26	1.21(1)
O26	C26	1.34(1)	O31	C31	1.29(1)
O33	C31	1.22(1)	O32	C32	1.28(1)
O34	C32	1.25(1)	O35	C36	1.24(1)
O36	C36	1.27(1)	N1	C13	1.50(1)
N1	C14	1.47(1)	N1	C15	1.50(1)
N2	C23	1.50(1)	N2	C24	1.50(1)
N2	C25	1.50(1)	N3	C33	1.52(1)
N3	C34	1.46(1)	N3	C35	1.52(1)
C1	C2	1.33(2)	C11	C13	1.52(2)
C12	C14	1.52(2)	C15	C16	1.50(1)
C21	C23	1.49(2)	C22	C24	1.50(2)
C25	C26	1.54(1)	C31	C33	1.52(2)
C32	C34	1.51(2)	C35	C36	1.53(2)

3.5. Mechanism for the formation of cluster 3

We propose the following reaction mechanism for the formation of **3**, as shown in Scheme 2. The reaction of **1** with ADA gives **1a** having two C–S bonds and shows an absorption peak at 853 nm. Lowering the pH causes the scission of one of the C–S bonds to give **1b**, and the addition of another ADA to **1b** gives the final product **3**. This mechanism is similar to that for the formation of the acetylene adduct of the tungsten cluster, $[W_3(\mu_3\text{-}S)(\mu_3\text{-}SCH{=}CHS)(\mu\text{-}SCH{=}CH_2)(NCS)_9]^{4-}$, ob-

Table 3
Bond angles (°) in $K_2[Mo_3(\mu\text{-}S)(\mu_3\text{-}S)(\mu_3\text{-}SCH{=}CHS)(Hnta)_3]\cdot KCl\cdot 8\ H_2O$ (**2′**)

Atom	Atom	Atom	Angle (°)	Atom	Atom	Atom	Angle (°)
Mo2	Mo1	Mo3	57.87(3)	Mo1	Mo2	Mo3	60.79(3)
Mo1	Mo3	Mo2	61.33(3)	S1	Mo1	S2	109.36(9)
S1	Mo1	S4	109.77(10)	S2	Mo1	S4	85.74(9)
S1	Mo2	S2	106.30(9)	S1	Mo2	S3	109.06(10)
S2	Mo2	S3	92.80(10)	S1	Mo3	S3	108.92(9)
S1	Mo3	S4	106.58(9)	S3	Mo3	S4	92.37(10)
Mo1	S1	Mo2	72.78(8)	Mo1	S1	Mo3	72.23(8)
Mo2	S1	Mo3	69.35(8)	Mo1	S2	Mo2	69.93(7)
Mo2	S3	Mo3	70.22(8)	Mo1	S4	Mo3	70.15(8)
Mo1	S2	C1	105.2(4)	Mo1	S4	C2	104.9(4)
Mo2	S2	C1	110.0(4)	Mo3	S4	C2	110.8(4)
S2	C1	C2	121.4(9)	S4	C2	C1	122.1(9)
O11	Mo1	O12	81.3(3)	O11	Mo1	N1	76.1(3)
O12	Mo1	N1	75.9(3)	O21	Mo2	O22	83.8(3)
O21	Mo2	N2	74.9(3)	O22	Mo2	N2	77.7(3)
O31	Mo3	O32	82.6(3)	O31	Mo3	N3	76.4(3)
O32	Mo3	N3	76.6(3)				

tained from the reaction of $[W_3(\mu_3\text{-}S)(\mu\text{-}S)_3(NCS)_9]^{5-}$ with acetylene via two intermediates, $[W_3(\mu_3\text{-}S)(\mu\text{-}S)(\mu_3\text{-}SCH{=}CHS)(NCS)_9]^{5-}$ having two C–S bonds and $[W_3(\mu_3\text{-}S)(\mu\text{-}S)_2(\mu\text{-}SCH{=}CH_2)(NCS)_9]^{4-}$ having one C–S bond [4]. The C–S bonds in $[Mo_3(\mu_3\text{-}S)(\mu_3\text{-}SCH{=}CHS)(\mu\text{-}X)(H_2O)_9]^{4+}$ (X = O, S) formed by the reaction of molybdenum aqua clusters $[Mo_3(\mu_3\text{-}S)(\mu\text{-}X)(\mu\text{-}S)_3(H_2O)_9]^{4+}$ (X = O, S) resist the attack of the H^+: exchanges of the aqua ligands for Hnta ones and the acetylene for ADA seem to make the C–S bonds more sensitive to H^+. We were unable to isolate **1a** as a solid sample.

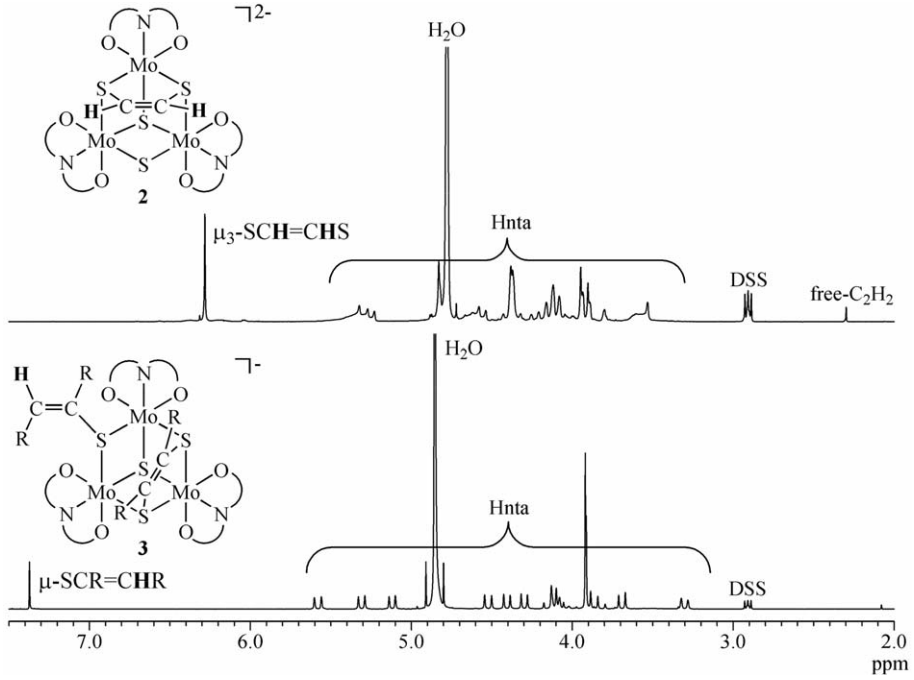

Fig. 4. ^1H NMR spectra of **2′** and **3′** (D_2O, 25 °C, 400 MHz).

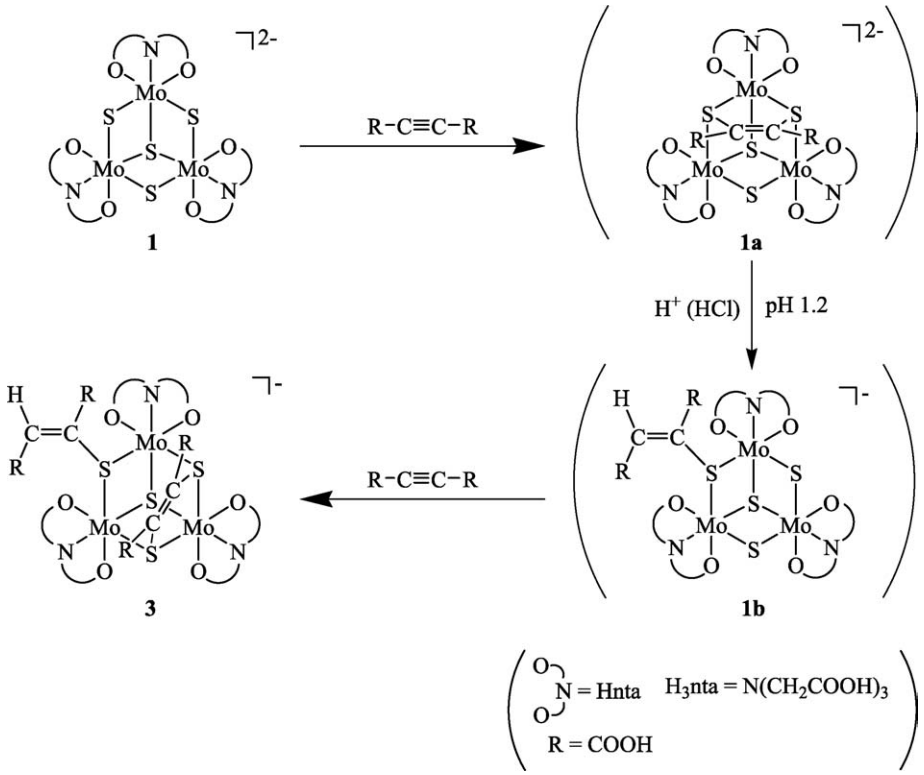

Scheme 2. Reaction mechanism of **1** with ADA.

*3.6. Electrochemistry of clusters **2** and **3***

As shown in Fig. 5, a one-electron reduction ($E_{1/2}$ = –0.68 V vs. Ag/AgCl) of **2** in a phthalate buffer solution at pH 4 was observed, and the potential was close to the first reduction potential of **1** [5]. The second and third reduction processes were not observed due to the hydrogen generation. Both reduction processes were assumed to undergo more negative potentials than those of **1**. This suggests that an adduction of acetylene to **1** has little influence on the reduction potential. Further, cluster **2** showed a one-electron oxidation at $E_{1/2}$ = +0.26 V, whereas no oxidation of **1** was observed. For the anodic process of **2**, the ratios between the current of the reverse peak and that of the forward peak, i_{pr}/i_{pf}, were 0.66 (the dotted line) and 0.52 (the solid line) at the scan rate v = 100 mV s^{-1} and 0.95 at the scan rate v = 500 mV s^{-1}. Therefore, the electrogenerated $\mathbf{2}^{+}$ is supposed to be unstable on the voltammetric timescale, and the anodic processes observed in the region greater than +0.5 V may be attributed to those of the oxidized products of the subsequent chemical reaction. In addition, the $E_{1/2}$ values obtained from cyclic voltammograms of **2** in pH 4 (a phthalate buffer solution) and pH 7 (a phosphate buffer solution) were not different from each other, and no protons participated in these redox reactions. In addition, in the basic solutions (pH > 7), the solution changed from deep green to colorless in 6 h. As a result, cluster **2** was unstable, and it was difficult to measure more negative

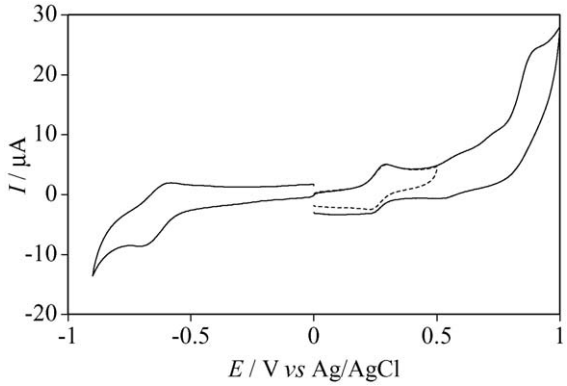

Fig. 5. Cyclic voltammograms of **2′** at pH 4. Scan rate 100 mV s^{-1}. Switching potential: dotted line E = 0.50 V.

potential regions in the basic solutions to avoid the hydrogen evolution.

It has been reported that incomplete cubane-type sulfur-bridged trinuclear molybdenum and tungsten clusters $[M_3S_4(Hnta)_3]^{2-}$ (M = Mo, W) containing only Hnta ligands have no anodic processes, while $[Mo_3S_4(Cp')_3]^+$ [11] and $[Mo_3S_4(CN)_9]^{5-}$ [12] containing 1-methyl cyclopentadienyl (Cp′) or CN^- ligands show anodic processes at $E_{1/2}$ = +1.22 V (+1.43 V) and + 0.25 V (+0.46 V vs. F_c/F_c^+) vs. Ag/AgCl in aprotic media, respectively. Both ligands in these clusters have no redox active site, and the anodic processes are suggested to occur in the metal centers.

In the case of acetylene adduct **2**, which has a partial dithiolene moiety, the anodic process is assumed to take place either in the ligand sites, as observed in dithiolene complexes [13], or in the metal center, with the oxidation number changing from Mo_3(IV, IV, IV) to Mo_3(IV, IV, V). Usually, an oxidation reaction of a dithiolene moiety in a complex proceeds via two consecutive one-electron oxidation processes from ene-1,2-dithiolate via 1,2-dithione monoanion to 1,2-dithione (Scheme 3): the two-electron oxidation product of complex $[Ni^{II}(S_2C_2Me)_2]^{2-}$, for instance, is $[Ni^{II}(S_2C_2Me)_2]$ with two ene-1,2-dithiolate ligands. The oxidation potentials between the complexes without redox active ligands vary according to the ligands. The oxidation potential of $[Mo_3S_4(CN)_9]^{5-}$ is close to that of **2**, and the reduction potential is 1.0 V more negative ($E_{1/2}$ = –1.70 V vs. Ag/AgCl) than that of cluster **2**. The difference in these redox potentials suggests that the electronic structure of $[Mo_3S_4(CN)_9]^{5-}$ is quite different from that of **2**. $[Mo_3S_4(Cp')_3]^+$, whose reduction potential is close to that of **2** ($E_{1/2}$ = –0.78 V vs. Ag/AgCl), is assumed to have a similar electronic structure and an oxidation potential that is more positive than that in cluster **2**. These results suggest that the oxidation of **2** occurs not at the molybdenum center but, rather, at the dithiolene moiety. No redox reaction processes of **3** at pH 4 and 7 were observed from the cyclic voltammetry measurements. The broad curves observed suggest that cluster **3** may be easy to adsorb on the electrode surface.

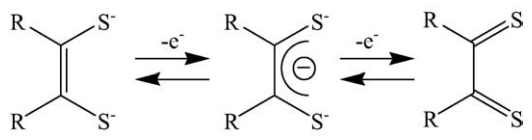

Scheme 3. Redox sequence of 1,2-dithiolene, 1,2-dithiolene monoanion, ene-1,2-dithiolene.

4. Supplementary material

Crystallographic data of **2′** (CCDC No. 244413) and experimental details of the synthesis and characterization (NMR and UV/Vis) of **2′** and **3′**.

Acknowledgments

This work was partly supported by a Grant-in-Aid for Scientific Research on Priority Areas (No. 14044110) ‘Exploitation of Multi-Element Cyclic Molecules’ and by a Special Grant for Cooperative Research administered by the Japan Private School Promotion Foundation. We thank the Research Instruments Center, Okayama University of Science, for permitting the use of instruments, and Ms. Rika Kyan for the preparative work.

References

[1] M. Rakowski DuBois, Chem. Rev. 89 (1989) 1.
[2] T. Shibahara, G. Sakane, S. Mochida, J. Am. Chem. Soc. 115 (1993) 10408.
[3] M. Maeyama, G. Sakane, R. Pierattelli, I. Bertini, T. Shibahara, Inorg. Chem. 40 (2001) 2111.
[4] Y. Ide, M. Sasaki, M. Maeyama, T. Shibahara, Inorg. Chem. 43 (2004) 602.
[5] T. Shibahara, M. Yamasaki, G. Sakane, K. Minami, T. Yabuki, A. Ichimura, Inorg. Chem. 31 (1992) 640.
[6] H. Takagi, A. Ichimura, T. Shibahara, Inorg. Chem. Commun. 2 (1999) 158.
[7] SIR92, A. Altomare, M.C. Burla, M. Camalli, M. Cascarano, C. Giacovazzo, A. Guagliardi, G. Polidori, J. Appl. Crystallogr. 27 (1994) 435.
[8] PATTY, DIRDIF94, P.T. Beurskens, G. Admiraal, G. Beurskens, W.P. Bosman, R. de Gelder, R. Israel, J.M.M. Smits, The DIRDIF-94 program system, Technical Report of the Crystallography Laboratory, University of Nijmegen, The Netherlands, 1994.
[9] Crystal structure Analysis Package, Molecular Structure Corporation: The Woodlands, TX, 1985 and 1992.
[10] M. Yamasaki, T. Shibahara, Anal. Sci. 8 (1992) 727.
[11] K. Herbst, P. Zanello, M. Corsini, N. D’Amelio, L. Dahlenburg, M. Brorson, Inorg. Chem. 42 (2003) 974.
[12] K. Wieghardt, W. Herrmann, A. Müller, W. Eltzner, M. Zimmermann, Z. Naturforsch. 39b (1984) 876.
[13] P. Zanello, in: Inorganic Electrochemistry, Chapter 6, Metal Complexes Containing Redox-active Ligands, Royal Society of Chemistry, London, 2003, p. 325.